

Kinetic study of Si recrystallization in the reaction between Au and polycrystalline-Si films

L. H. Allen and J. W. Mayer

Department of Materials Science and Engineering, Cornell University, Ithaca, New York 14853

K. N. Tu

IBM, Thomas J. Watson Research Center, Yorktown Heights, New York 10598

L. C. Feldman

AT&T Bell Laboratories, Murray Hill, New Jersey 07974

(Received 23 June 1989; revised manuscript received 13 September 1989)

The kinetics of Si crystallization during isothermal annealing of Au/polycrystalline-Si bilayers were investigated via scanning electron microscopy and *in situ* sheet-resistance measurements. Large crystals of Si grow within the Au layer in the shape of two-dimensional plates of thickness equal to that of the Au layer. The Si crystals grow at an average rate which follows a t^2 time dependence with an Arrhenius temperature dependence of $\tau \propto e^{E_\tau/kT}$, where $E_\tau \approx 2.4$ eV. The overall transformation rate is a product of the two separable processes: the first determines the number of crystals and the second the growth rate of the crystals. At the beginning of the reaction the number of crystals, N , per unit area is fixed, remains constant throughout the anneal, and has an Arrhenius temperature dependence of $N \propto e^{-E_N/kT}$ where $E_N \approx 1.0$ eV. The crystals grow at a constant growth rate and have an Arrhenius temperature dependence of $v \propto e^{-E_v/kT}$ with $E_v \approx 1.9$ eV. Final analysis of the overall transformation relates the activation energy of the total process to the activation energy of adding or removing an atom from the Si surface (E_v) and the diffusion of Si in Au (E_D): $E_\tau = \frac{3}{2}E_v - \frac{1}{2}E_D$.

I. INTRODUCTION

The formation of large Si crystals has been observed¹ during thermal anneals of Au/polysilicon (where polysilicon denotes polycrystalline Si) bilayers. These Si crystals are formed at much lower temperatures ($T \approx 300^\circ\text{C}$) than the typical recrystallization temperature² of polysilicon (1000°C) without gold. Experiments have shown that Si dissolves into Au and diffuses rapidly through Au at temperatures well below the Au/Si eutectic³ (365°C) to achieve recrystallization.

It was shown in the accompanying paper¹ that thermal annealing of Au/polysilicon bilayers produced flat, two-dimensional Si crystals (*c*-Si), of thickness equal to the thickness of the original Au layer.

These crystals are the result of the growth of an already existing grain located at the initial Au/polysilicon interface which grows upward into the Au until impinging the top surface, and then grows radially in the shape of a two-dimensional platelike crystal. Supply of Si from the surrounding polysilicon layer to the crystals occurs through the long-range transport of Si through the Au layer. One-to-one displacement of the Au by the Si keeps the total thickness of the sample constant and uniform. The final configuration consists of a top layer of large Si crystal plates on a composite layer of Au and polysilicon, where the Au is distributed in a network of spikes and sublayers within the polysilicon layer.

This work investigates quantitatively the growth kinetics of the Si crystals by *in situ* sheet-resistance measurements⁴ and scanning-electron-microscopy (SEM) measurements.

II. EXPERIMENT

Polysilicon thin films, 4500 Å thick, were deposited via a low-pressure chemical-vapor-deposition (LPCVD) process at 620°C , on thermally oxidized single-crystal Si wafers. TEM cross sections and x-ray diffraction (XRD) of these films indicated that the grains were columnar and had [110] fiber texture.¹

A total thickness of 2500 Å of Au was deposited onto the polysilicon films via resistive thermal evaporation with base pressure of 5×10^{-6} Torr. Samples were subsequently annealed in a vacuum furnace at a pressure of 1×10^{-7} Torr. The temperature control had a precision of $\pm 0.5^\circ\text{C}$.

Sheet-resistance measurements were obtained *in situ* via a Van der Pauw-type arrangement of four molybdenum spring-loaded probes. A JEOLTM 35 scanning electron microscope was used to obtain images of the Si crystals, and quantitative dimensions of the crystals were obtained via image-processing techniques. Rutherford backscattering spectroscopy (RBS) was used to determine the thickness of the Si and Au films.

III. RESULTS

A. Sheet-resistance measurements

When Au/polysilicon bilayers are isothermally annealed (Fig. 1), the sheet resistance $R(t)$ of the sample increases with time. In order to relate the changes in resistance to the kinetic process of the reaction, we adopt a physical model which represents the sample as two regions: the top region, outlined by the original Au film, and the bottom region, framed by the original polysilicon film. Initially, the top region contains only Au; the volume fraction of Si in this region is zero. As the reaction proceeds and the Au is replaced by the formation of isolated Si grains, the layer becomes progressively more resistive. The bottom layer, which was initially electrically semiconducting, becomes more conductive with the anneal, as the displaced Au penetrates the polysilicon, forming a complex, conductive network of vertical spikes and sublayers. Since Au and Si are immiscible at these temperatures, the Au and Si remain separate. The redistribution changes the geometry of the effective conductive path, which results in the increase of the overall resistance.

The reacted system is quantitatively related to the measured resistance by modeling the top and bottom regions of the sample as two parallel resistors. The conductance of each region is assumed to be proportional to the amount of Au in each region. By coupling the conductance of the two regions via conservation of Au, we can relate the volume fraction X_R of Si crystals in the top Au layer with the measured resistance $R(t)$,

$$X_R(t) = \frac{R_0 - R(t)}{R_0 - R_F} \frac{R_F}{R(t)} \quad (1)$$

in terms of the initial (R_0) and final (R_F) values of resistance.

Equation (1) can be applied directly for analyzing a

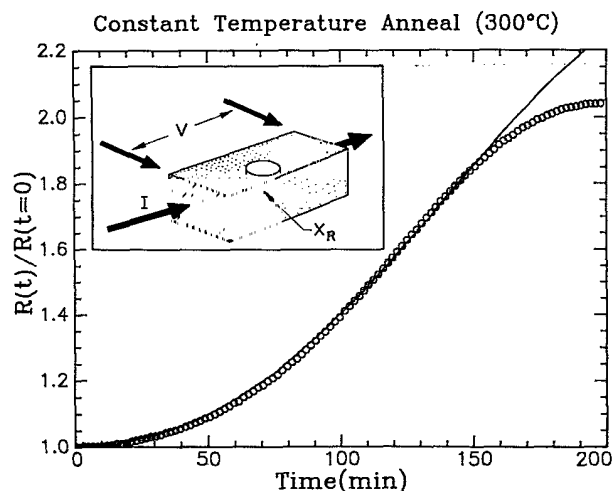


FIG. 1. Normalized resistance measured *in situ* during 300°C isothermal annealing. Solid line represents the model [Eqs. (1)–(3)], with $n=2.0$, $R_0/R_F=2.5$, and $\tau=87.7$ s. The inset represents the effective model of the measurement.

layer-by-layer growth process,⁵ where $X_R(t)$ would be proportional to the thickness of the growing layer. However, Eq. (1) must be modified in the latter stages of the reaction, in systems where crystal growth is influenced by the impingement of adjacent crystals and percolation prevails. The transformed fraction $X_{R'}$ of the reaction which includes impingements is related to the actual volume (area) fraction X_R by using the Avrami equation,⁶

$$X_R = 1 - e^{-X_{R'}} \quad (2)$$

At the initial stage of the reaction, where there is no impingement, $X_{R'}$ is small, and so $X_R \approx X_{R'}$.

Equations (1) and (2) were applied to the resistance data in order to obtain the time dependence of the transformed crystal volume fraction $X_{R'}$ in the initial stage. The parameter R_F was used as a fitting parameter in Eq. (1), because the final resistance of the system was not well defined, since the resistance continued to change even after the reaction was completed due to further redistribution of the Au in the underlying layer of crystal platelets. By plotting the resistance data (Fig. 1) in the form of $\ln(X_{R'})$ versus $\ln(t)$ (Fig. 2), we observe the general relationship

$$X_{R'} = \frac{1}{2}(t/\tau)^n \quad (3)$$

where τ is a time-independent constant. A value of $n \approx 2.1$ was obtained from the slope of the curve, indicating that the reaction proceeds with approximately a t^2 dependence. A comparison of the calculated time dependence using Eq. (1) ($n=2$ and $R_F/R_0=2.5$) are compared with original data in fig. 1 and shows good agreement through $\approx 80\%$ of the reaction.

The parameter n is the mode parameter in the reaction process; it can have various values depending on the rate-limiting process(es) in the system. Tables generated by theoretical models have yielded various values of n for particular combinations of nucleation and growth processes.^{7–9} For example, in the case of a constant number

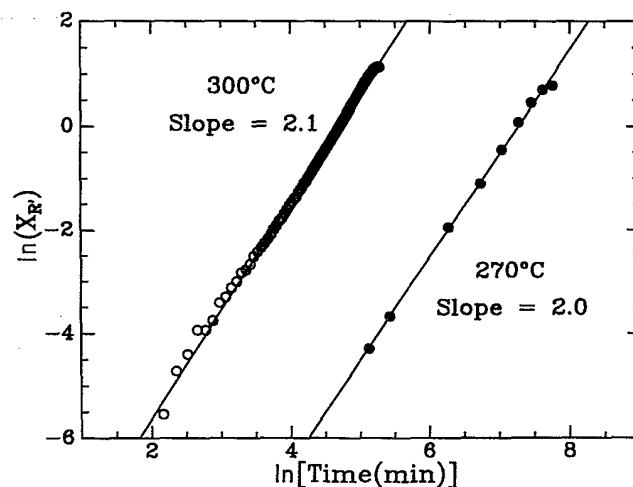


FIG. 2. Resistance data from Fig. 1 reduced to a form which accounts for crystal impingement. The plot of $\ln(X_{R'})$ vs $\ln(t)$ indicates the relationship $X_{R'} \propto t^n$, where $n=2.1$ is the slope.

of spheres growing in a three-dimensional manner, where the interface (surface of the sphere) limits the rate of growth, the time dependence would be t^3 ($n=3$). In the two-dimensional case, where plates are growing, the time dependence would be t^2 ($n=2$). However, we cannot uniquely identify the rate-controlling process based solely on the value of n , since multiple processes (i.e., growth and nucleation) may individually control the rate of reaction. Although the origin of crystals is due to grain growth and not to nucleation, this does not preclude the possibility of the number of grains changing during the anneal. In order to separate the time-dependent effects of growth from the number of crystals, we measured the number and volume (area) of the crystals using SEM.

B. SEM measurements

The growth process of Si crystals was measured directly via SEM analysis. The Si crystals in the top layer were easily observed by SEM, appearing as dark patches in the film. The data presented in this subsection were obtained from different samples from the same substrate. Each sample was isothermally annealed only once, at a specific temperature (T) for a given anneal time (t). The number of crystals, as well as their size, were measured using the image-processing capabilities of the SEM system. The average crystal size was determined by dividing the fraction of the area covered by crystals by the total number of crystals. Data collection was limited to the first 30% of the reaction so as to avoid significant crystal impingement. During the first 30% of the reaction, the crystals were observed to grow independently of each other.

SEM micrographs (shown in Fig. 3) were obtained

from samples annealed isothermally at 270 and 290°C for various anneal times. We first investigate the number of crystals during the anneal. The average number (N) of crystals versus anneal time is plotted (Fig. 4) for two (270 and 290°C) anneals. The data indicate that at a given temperature the number of crystals is fixed at the beginning of the reaction and does not appreciably change during the anneal. However, the number of crystals does depend on temperature, $N(T)$. The average number of crystals during the 290°C anneal ($\approx 0.07/\mu\text{m}^2$) is 3 times higher than the number observed during the 270°C anneal ($\approx 0.02/\mu\text{m}^2$).

Although the number of crystals does not change during the anneal, the crystal area increases significantly with time. The average crystal area is plotted as a function of time (Fig. 5) for anneals at 270 and 290°C. The data indicate that at the early stages of the reaction ($< 50\%$) there is a linear relationship between the square root of the crystal area (A) and time t ,

$$A^{1/2} = \pi^{1/2} vt \quad (4)$$

The factor v , referred to as the linear growth rate (velocity), is constant, and is obtained by measuring the slope of the $A^{1/2}$ -versus- t curve. The parameter $v(T)$ does depend on the anneal temperature, increasing from 0.2 Å/s at 270°C to 1.25 Å/s at 290°C.

C. Temperature dependence of growth rate v and number of crystals N

To determine the temperature dependence of $N(T)$ and $v(T)$, the crystal area and the number of crystals were

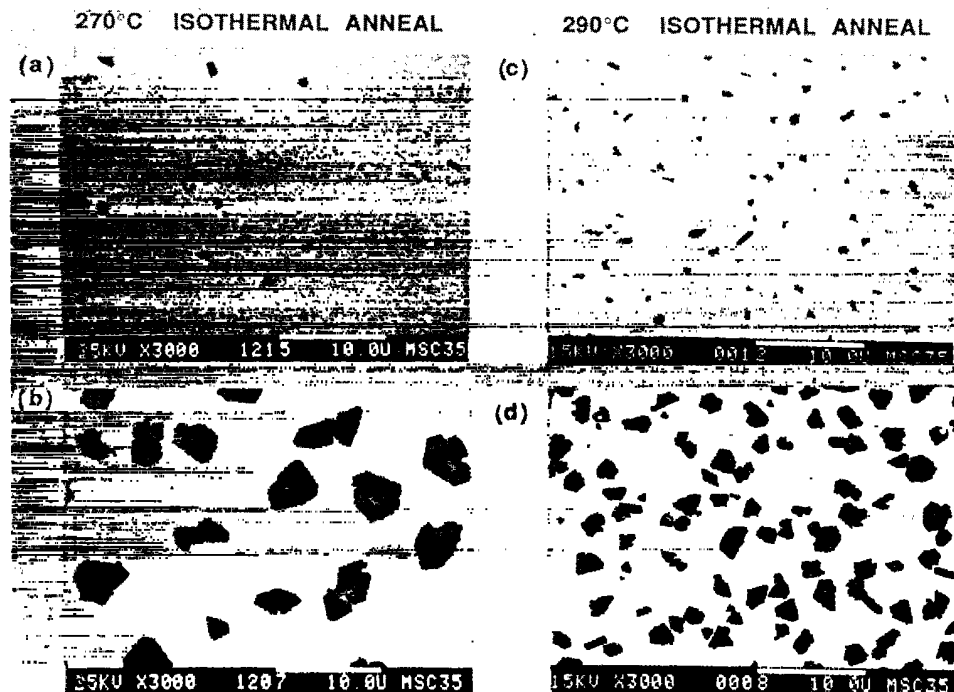


FIG. 3. SEM micrographs of four different samples annealed at (a) 270°C (380 min), (b) 270°C (1900 min), (c) 290°C (76 min), and (d) 290°C (196 min).

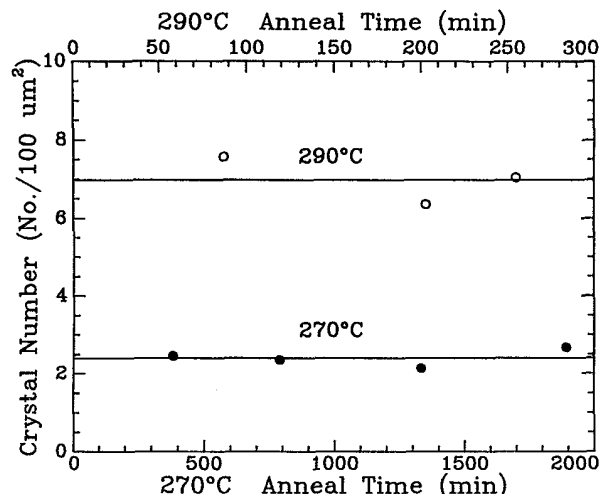


FIG. 4. Number of crystals per unit area (N) as a function of annealing time and temperature. The 290°C anneal is plotted vs time on the top axis, and the 270°C anneal vs time on the bottom axis.

measured over a range of temperatures. The data shown in Figs. 6(a) and 6(b) indicate that both parameters follow the Arrhenius-type relation, $N(T) = N_0 e^{-E_N/kT}$ and $v = v_0 e^{-E_v/kT}$, where N_0 and v_0 are constants. Two separate activation energies ($E_N = 1.0$ eV and $E_v = 1.9$ eV) were experimentally determined from the data. The activation energy E_N is associated with the number of crystals at a given temperature, and E_v is associated with the crystals-growth rate at a given temperature.

Having analyzed the reaction in terms of the individual process components, the crystal number (N) and growth rate (v), we can now construct an expression for the reaction. The total area fraction X_{SEM} of the surface covered by the crystals at any time and temperature as determined from SEM data can be expressed as the product of

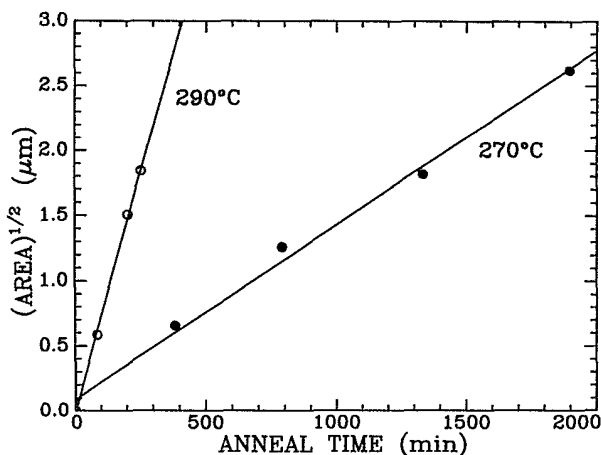


FIG. 5. Growth rate plotted as the square root of the average crystal area ($A^{1/2}$) vs annealing time at two (270 and 290°C) temperatures.

the number (N) of the crystals per unit area and the average area (A) per crystal:

$$X_{SEM} \equiv N(T) A(T, t). \quad (5)$$

By using the experimentally determined relationships between the parameters, X_{SEM} can be expressed explicitly in terms of time and temperature as

$$X_{SEM}(T, t) = \pi N_0 v_0^2 e^{-(E_N + 2E_v)/kT} t^2. \quad (6)$$

The results obtained from the SEM data can be summarized as follows. The accumulative process of replacing the Au layer with Si crystals is a product of two separate factors: the number of crystals, which is independent of time but thermally activated, and the crystal-growth process, which has a given ($A^{1/2} = \pi^{1/2} v t$) time dependence where the rate constant v is time independent but thermally activated.

D. Comparison of resistance and SEM results

In this subsection we compare the results obtained from the SEM data with the resistance data. This is ac-

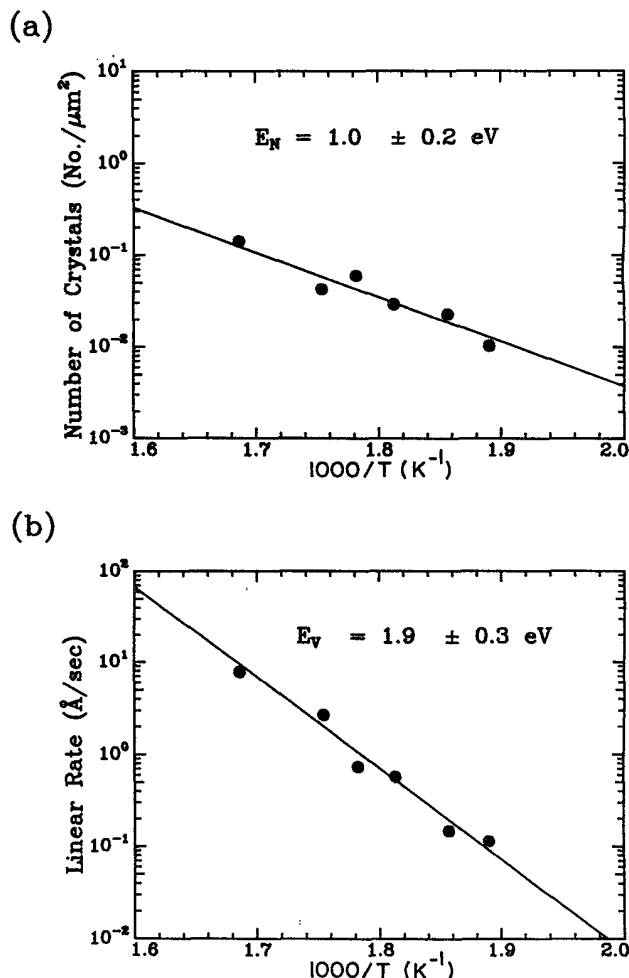


FIG. 6. (a) Number (N) of crystals per unit area, and (b) linear rate of growth (v), plotted vs $1000/T$ (K^{-1}).

completed by utilizing a parameter τ , which can be related to both resistance and SEM measurements. The parameter τ is defined as the time of anneal at which the reaction is 50% completed. For the resistance measurements, τ_R is extracted directly from the data, with the requirement that $X_R = \frac{1}{2}$. In the case of the SEM data, τ_{SEM} is calculated from the SEM data using the relation $\tau_{SEM} = (2\pi N v^2)^{1/2}$, which is derived from Eqs. (4) and (5), with the condition that $X_{SEM}(t = \tau) = \frac{1}{2}$. The values for τ_{SEM} and τ_R obtained from both SEM and resistance data are plotted together in Fig. 7, and show good agreement. This confirms the claim that the methods, although independent of each other, are equivalent [$X_{SEM}(t) \approx X_R(t)$]. The difference is that the SEM measurement is able to separate the overall process of transformation into its components.

The resistance and SEM data shown in Fig. 7 correspond to an Arrhenius plot with a characteristic activation energy. Typically, the characteristic activation energy of a system is analyzed via an Arrhenius plot (Fig. 7), by measuring the slope of the data and using the general phenomenological relation

$$\tau = \tau_0 e^{E_\tau / kT}, \quad (7)$$

where τ_0 is temperature independent. From the analysis of the data, we obtain values of $E_{\tau_{SEM}} \approx E_{\tau_R} \approx 2.4$ eV for the activation energies measured by two the independent methods. This specific activation energy represents the activation energy of the entire process.

E. Comparison of activation energies

It is useful to relate the phenomenological parameter $E_{\tau_{SEM}}$ with the specific process which determines the number of crystals (E_N) and the process of grain growth (E_v). Since the activation energy $E_{\tau_{SEM}}$ was obtained from the same set of data as the values E_N and E_v , it is not surprising that the parameters depend on one another.

er. The relationship between the activation energies can be derived by evaluating Eq. (6), and setting $X_{SEM} = \frac{1}{2}$ at time $t = \tau_{SEM}$:

$$\tau_{SEM} = (2\pi N_0 v_0^2)^{-1/2} \exp[-(E_N + 2E_v) / 2kT]. \quad (8)$$

Given that the phenomenological relation is defined by $\tau_{SEM} = \tau_{0SEM} \exp(E_{\tau_{SEM}} / kT)$, the expression in Eq. (8) can be further reduced to the following equation:

$$E_{\tau_{SEM}} = \frac{1}{2}E_N + E_v - \frac{1}{2}kT \ln(2\pi N_0 v_0^2 \tau_{0SEM}^2). \quad (9)$$

Since all of the parameters $E_{\tau_{SEM}}$, E_N , E_v , N_0 , v_0 , and τ_{0SEM} are temperature independent, it can be shown that the term $\frac{1}{2}kT \ln(\dots)$ in Eq. (9) will be zero, and therefore

$$E_{\tau_{SEM}} = \frac{1}{2}E_N + E_v. \quad (10)$$

To confirm this result, values for E_N and E_v have been compared with E_τ [$E_{\tau_{SEM}} = (1.0/2 + 1.9)$ eV = 2.4 eV] and again show good agreement.

The factor 2 in Eq. (10) is a consequence of the growth mode of the system. In general, given a reaction of interface-limited growth with instantaneous nucleation (or, as in our case, a constant time-independent number of crystals), the factor will equal the number of degrees of freedom of growth. This factor would be equal to 3 if the crystals were growing in three dimensions, and would be 1 if the crystals were limited to one-dimensional (1D) growth.

F. Effects of various poly-Si substrates

The rates of the reaction for three separate polysilicon substrates (LPCVD, 620°C) are plotted in Fig. 8 in terms of the parameter τ . The data show that the reaction rate varies considerably, by a factor of ≈ 50 , from one substrate to another, although the activation energies are comparable ($E_\tau = 2.13, 3.21, \text{ and } 2.38$ eV). It was determined from several measurements that the variation in

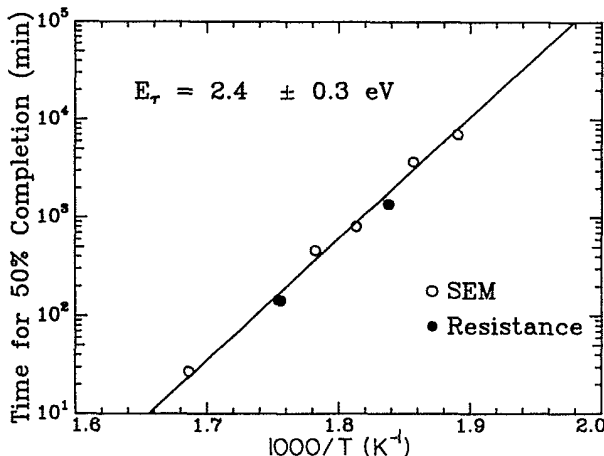


FIG. 7. Values of τ vs $1000/T$ (K^{-1}) from resistance (\bullet) and SEM (\circ) data are compared. The parameter τ is the time it takes for the reaction to proceed to 50% of completion.

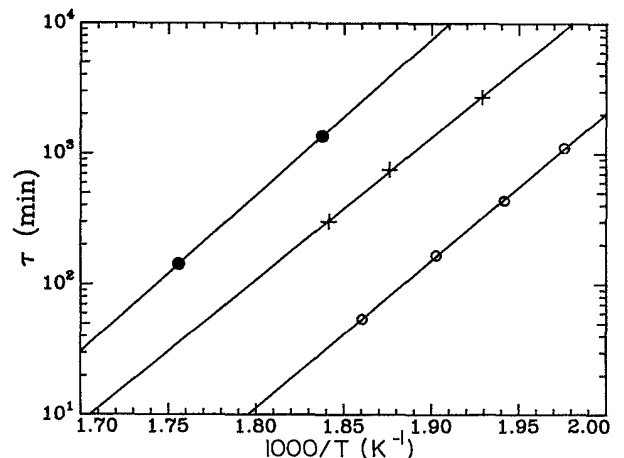


FIG. 8. Reaction rate in terms of τ [$X_R(\tau) = \frac{1}{2}$] is plotted vs $1000/T$ (K^{-1}) for three different polysilicon substrates.

reaction rates is mainly due to variations in the polysilicon deposition: substrates within a particular deposition batch gave similar reaction rates. On the other hand, the variation in the Au-deposition process did not produce significant variations in the reaction rate.

IV. DISCUSSION

The growth of Si crystals is a thermally activated process, with the rate of the total transformation proportional to $\exp(E_\tau/kT)$. Because the crystals are large and separated from each other, it is possible to describe the total transformation as a product of two processes which control the number of crystals and their growth rate. This discussion analyzes the time and temperature dependence of each process and relates the individual activation energy (E_v and E_N) to basic physical mechanisms.

Individual Si crystals grow at a rate which has an activation energy of $E_v = 1.9$ eV. The number of growing crystals is fixed at the beginning of the reaction and remains the same throughout the anneal, but the number of crystals depends on the temperature of the isothermal anneal, having a activation energy $E_N \approx 1.0$ eV. The relationship among these activation energies is given as $E_\tau = E_v + E_N/2$.

The rate of growth of the crystal area was established by experimental data as $A^{1/2} = \pi^{1/2}vt$. If the crystals had the shape of circular disks, the parameter v ($\mu\text{m}/\text{min}$) would be easily interpreted as a constant growth velocity of the circumference of the crystal. Since the crystals in this study have faceted shapes, a simple relationship between v and the growth rate of the edges of the crystal cannot be directly established. The physical meaning of v is assumed to be an average velocity of all the edges of the crystal, each growing at a constant rate.

The condition of a constant growth rate that is independent of crystal size and shape is consistent with an interface-limited growth process. Therefore we conclude from this result that the growth of the crystal is limited by the interface (Au/c-Si) and is not limited by the diffusion of Si through the Au.

Since the number of crystals does not change during the reaction, we can further evaluate the reaction-rate parameter n [Eq. (3)] obtained from the resistance data. From Dormeus⁷ the factor n would have values of $\frac{1}{2}$ (plate-shaped crystals) or $\frac{3}{2}$ (spherical-shaped crystals) in a diffusion-limited growth mode. If the system was controlled by an interface-limited process, the factor n would have a value of 2 (plate-shaped crystals) or 3 (spherical-shaped crystals). The measured value of n in this study was 2.1, which agrees with previous analysis in that the reaction is controlled by the interface-limited growth of plate-shaped crystal.

This localized interface process is speculated to be a process of fitting an atom to the growing interface of the crystal. The activation energy $E_v \approx 1.9$ eV is associated with growing a Au/c-Si interface. We expect the energy E_v to be 2 eV or slightly higher since it should be close to the energy needed to add or remove a Si atom from a low-index surface of Si crystal.¹⁰

Although diffusion does not limit the growth rate of

the crystals, it does play a key role in determining the distance between the crystals, which will be discussed later.

An interesting result for Au/polysilicon is the unusually large size of the Si crystals. Since the size of the crystals is inversely proportional to the number of the crystals, N , it is useful to discuss those factors that may control the value N . Two key results of this investigation are that the number of growing crystals is fixed at the initial stage of the reaction and that this number is time independent. The origin of these crystals has been investigated,¹ and it was concluded that each crystal is the result of the growth of an already existing grain located at the initial Au/polysilicon interface which grows in a 3D manner until impinging the top surface, and then grows in a 2D manner radially to form two-dimensional plate-like crystals. The growing Si crystal displaces the Au. Given the wide initial distribution of grain sizes² at the interface, only the larger grains are expected to grow (Ostwald ripening). These grains grow at the expense of the smaller grains. The relationship between the driving force for growth and the size of the grain is a simplification of the Thomson-Freundlich relation, which relates the driving force in the system to the radius of curvature of the particle. Since the polysilicon is an accumulation of columnar grains with a wide variation of diameters, we assume the simple relationship that the size and diameter of the grain is directly (inversely) related (on the average) to the curvature of the exposed surface.

Ideally, there would be only one largest grain for the entire sample, and this grain would grow at the expense of all other grains, which dissolve into the Au at a rate prorated according to their size, but the diffusivity of Si in Au is finite and thus restricts the transport of Si from distances far away from the growing crystal. The area from which the crystal draws the Si is limited to the immediate vicinity of the crystal. The extent of this affected area depends on two factors: the local dissolution rate of the polysilicon crystals, and the diffusion of Si through Au. The size of this local region determines the final size and number of crystals.

Since the diffusivity of Si in Au is finite, there will be a concentration gradient of Si in the Au perpendicular to the growing interface. The dissolution rate of the polysilicon grains near the growing crystal will be higher than those far away from the crystal. This was verified from TEM data,¹ which clearly shows that more of the polysilicon grains were dissolved in the region near the crystal.

A quantitative analysis of the dissolution and diffusion of Si to the crystal is treated in the Appendix. From this analysis we obtain an expression for the radius (L) of the affected region,

$$L^2 \propto D/B, \quad (11)$$

in terms of the diffusion coefficient (D) of Si in Au and the average dissolution rate (B) of the polysilicon grains. This parameter L sets the initial boundaries of the affected area at the early stages (<5%) of the reaction. At the latter stages of the reaction the affected regions of the crystals will overlap, suppressing to an even greater extent the growth of other grains in the region between crystals. Therefore it is the initial value of L that deter-

mines the distance between the crystals (see Fig. 9) and, consequently, the number of crystals per unit area N , since

$$\pi L^2 \propto 1/N = \lambda_N D / B, \quad (12)$$

where λ_N is a constant. The value for N is expected to be constant throughout the anneal, as is experimentally observed.

Assuming a simple dependence of $B = \lambda_B \exp(-E_B/kT)$ and $D = \lambda_D \exp(-E_D/kT)$ on temperature T , where λ_B and λ_D are constants, it follows from Eq. (11) that

$$N_0 \exp(-E_N/kT) = (\lambda_B / \lambda_N \lambda_D) \exp(-E_B/kT) / \exp(-E_D/kT). \quad (13)$$

Since N_0 , λ_B , λ_N , λ_D , E_N , E_B , and E_D are all assumed to be temperature independent, it can be shown that $1 = \lambda_N \lambda_D N_0 / \lambda_B$, and we can set the coefficient of T (on each side of the equation) equal to each other,

$$E_N = E_B - E_D. \quad (14)$$

Consider the dissolution factor B , the rate at which Si atoms are removed from the small-grained Si. For a given crystal at equilibrium, the dissolution rate will equal the growing rate. It can also be shown that for the same crystal the activation energy of the growth rate is equal to the activation energy of the dissolving rate. We argue that the activation energy of the dissolution rate

E_B of the small-grained crystals will be approximately equal to the activation energy of the growth rate of the large-grained crystal (*c*-Si), E_v , since the chemical-potential difference of small versus large Si grains is small (± 0.1 eV).¹ Therefore we have

$$E_B \approx E_v \approx 1.9 \text{ eV}. \quad (15)$$

We could not obtain data regarding the activation energy E_D of Si in Au, so we assume a value¹¹ of $E_D \approx 0.8$ eV from the Al/Si system, which is another eutectic system that reacts with polysilicon in much the same way (Si crystal growth) as in the Au/Si system. Now we can evaluate the term E_N ($E_N = E_B - E_D \approx E_v - E_D \approx 1.1$ eV), and we find good agreement with the measured value ($E_N = 1.0$ eV).

At low temperatures the distance L_L will be large ($L^2 \propto \exp[(1.1 \text{ eV})/kT]$) and the largest crystal will dominate, suppressing the growth of all other crystals within the region. At higher temperatures L_H will be smaller and the affected region will also be smaller, allowing additional grains outside of this region to grow. This process is diagrammed in Fig. 9.

We conclude from this analysis that the thermal activation energy (E_τ) for the total transformation process depends on two basic processes: the exchange of Si atoms from the Si surface (E_v) and the diffusion (E_D) of Si through Au. By combining Eqs. (10), (14), and (15), E_τ can be rewritten explicitly in terms of E_v and E_D ,

$$E_\tau = \frac{3}{2} E_v - \frac{1}{2} E_D. \quad (16)$$

Large differences in transformation rates, but comparable activation energies, were observed in a given set of polysilicon samples. It is speculated (and qualitatively supported via x-ray data) that the difference in reaction rate from sample to sample is due to differences in the average grain size. The rate of reaction at any given temperature would be expected to be strongly dependent on microstructure (i.e., average size of grains). The driving force for this reaction, $\Delta\mu_{\text{Si}}$, depends strongly on particle size: the smaller the grains, the faster the reaction. The insensitivity of the activation energy to the type of polysilicon is expected since the basic mechanism (adding or removing Si atoms from Si, and Si diffusion in Au) are insensitive to polysilicon microstructure.

V. SUMMARY

This investigation characterizes the time and temperature dependences of the formation of Si crystals during isothermal anneals of Au/polysilicon bilayers by using *in situ* resistance measurements and SEM analysis.

This reaction is controlled by two separate processes: the growth rate of the individual crystals, and the total number of growing crystals. Individual Si crystals grow with an interface-limited growth process within the Au layer at a constant linear growth rate (v) with an activation energy of $E_v = 1.9$ eV. The number of growing crystals is fixed at the beginning and remains the same throughout the anneal, but the number of crystals depends on the temperature of the isothermal anneal, hav-

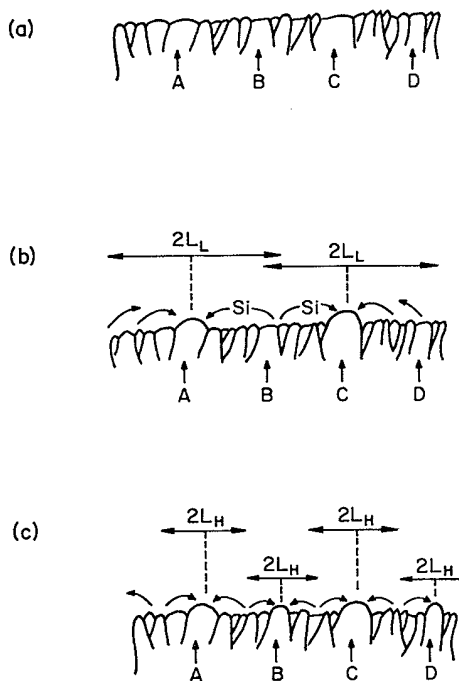


FIG. 9. Diagram of the initial stages of crystal growth with (a) no thermal annealing, (b) with low-temperature annealing (large diffusion length L_L), and (c) with high-temperature annealing (short diffusion length L_H). Note that only grains AC grow at low temperatures, while grains A-D grow at higher-temperature annealing.

ing an activation energy $E_N \approx 1.0$ eV. The relationship of these activation energies to the activation energy of the total reaction, E_τ , is given as $E_\tau = E_N/2 + E_v$.

The number of crystals during an isothermal anneal is determined by the dissociation constant of the fine-grained poly-Si and the diffusion coefficient of Si in Au.

Further analysis of these separate processes show that they can be related to the more basic processes: the process of adding or removing Si atoms from a Si surface, and the diffusion of Si in Au. The activation energy of the overall process can be written as $E_\tau = \frac{1}{2}E_v - \frac{1}{2}E_D$.

ACKNOWLEDGMENTS

This work was supported in part by IBM General Technologies Division (Dave Campbell and Evan Colgan), Hopewell Junction, NY, and by the Cornell Microscience Center of the Semiconductor Research Corporation. Special thanks are due to B. Soave for the deposition of the poly-Si films. We thank the staff of the Material Science and Engineering (MS&E) (John Hunt, Ray Coles and Margret Craft) microscopy facility for the use and instruction of their TEM and SEM equipment. We also express our gratitude to Larry Doolittle for his assistance in setting up the *in situ* resistance-measurement system.

APPENDIX

Here we model the region near the growing crystal, relating the dissolution rate (B) of the poly-Si and the diffusion coefficient of Si in Au (D) with the relative concentration (C) of Si in Au at a position (r) relative to the crystal position. It is assumed that the crystals have reached a steady-state rate of growth and that the size of the crystals is much less than the distance between the crystals.

Assume that the flux of Si, $J_z(r)$, dissolving from the poly-Si is linearly dependent on the deviation of the local Si concentration $C(r)$; we obtain the relation

$$J_z = B(C_0 - C), \quad (\text{A1})$$

where C_0 is the concentration far away from the crystal.

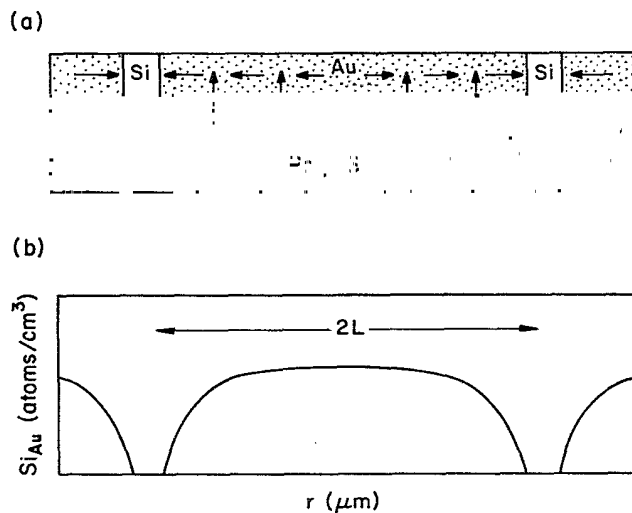


FIG. 10. (a) Diagram of the two-dimensional model describing the dissolution of Si from the poly-Si layer and the flow of Si toward the crystals. (b) Si concentration profile $C(r)$ within the Au.

The continuity equation

$$I'(r) = 2\pi r J_z \quad (\text{A2})$$

relates the total flux of Si, $I(r)$, to the local Si flux from the poly-Si, where $dI/dr = I'(r)$. Using Fick's first law,

$$J_r = -DC', \quad (\text{A3})$$

and the relation $I = 2\pi r d_{\text{Au}} J_r$, where d_{Au} is the gold thickness, we obtain the differential equation

$$C'' + C'/r - C/L^2 = -C_0/L^2. \quad (\text{A4})$$

The solution to this equation is a modified hyperbolic Bessel function $K_0(x/L)$, where $L^2 = d_{\text{Au}} D/B$, and C_0 is the Si concentration at the crystal edge r_0 . The factor L (μm) can be interpreted as an effective diffusion length. A plot of the Si concentration and fluxes for this model are given in Fig. 10.

¹L. H. Allen, J. R. Phillips, D. Theodore, J. W. Mayer, and G. Ottaviani, preceding paper, Phys. Rev. B **41**, xxxx (1990).

²T. Kamins, *Polycrystalline Silicon for Integrated Circuit Applications* (Kluwer, Boston, 1988).

³A. Hiraki, in *Progress in the Study of Point Defects*, edited by M. Doyama and S. Yoshida (University of Tokyo Press, Tokyo, 1977).

⁴S. Mader and A. S. Nowick, Acta Metall. **15**, 215 (1967).

⁵M. Avrami, J. Chem. Phys. **9**, 177 (1941).

⁶L. H. Allen and Q. Z. Hong, unpublished results on thermal

annealing of the Pt/Ge system.

⁷R. H. Doremus, *Rates of Phase Transformation* (Academic, Orlando, FL, 1985).

⁸J. W. Christian, *Transformation in Metals and Alloys* (Pergamon, New York, 1965).

⁹I. S. Servi and D. Turnbull, Acta Metall. **14**, 161 (1966).

¹⁰A. S. Grove, *Physics and Technology of Semiconductor Devices* (Wiley, New York, 1967), p. 29.

¹¹S. K. Ghandi, *VLSI Fabrication Principles* (Wiley, New York, 1983).